



Universiteit  
Leiden  
The Netherlands

## Regulators of growth plate maturation

Emons, J.A.M.

### Citation

Emons, J. A. M. (2010, April 14). *Regulators of growth plate maturation*. Retrieved from <https://hdl.handle.net/1887/15225>

Version: Corrected Publisher's Version

License: [Licence agreement concerning inclusion of doctoral thesis in the Institutional Repository of the University of Leiden](#)

Downloaded from: <https://hdl.handle.net/1887/15225>

**Note:** To cite this publication please use the final published version (if applicable).

10

# Fetal mesenchymal stem cells differentiating towards chondrocytes display a similar gene expression profile as growth plate cartilage.

**J.A.M. Emons<sup>1\*</sup>, S.A. van Gool<sup>1\*</sup>, J.C.H. Leijten<sup>2</sup>, E. Decker<sup>3</sup>, X. Yu<sup>4</sup>, C. Sticht<sup>4</sup>, J.C. van Houwelingen<sup>5</sup>, J.J. Goeman<sup>5</sup>, C. Kleijburg<sup>6</sup>, S. Scherjon<sup>6</sup>, N. Gretz<sup>4</sup>, J.M. Wit<sup>1</sup>, G. Rappold<sup>3</sup>, M. Karperien<sup>1,2</sup>.**

<sup>1</sup>Department of Pediatrics, Leiden University Medical Center, Leiden, the Netherlands;

<sup>2</sup>Department of Tissue Regeneration, Twente University, Enschede, the Netherlands;

<sup>3</sup>Department of Human Molecular Genetics, and

<sup>4</sup>Medical Research Center, Medical Faculty Mannheim, University of Heidelberg, Heidelberg, Germany;

<sup>5</sup>Department of Medical Statistics and Bioinformatics, and

<sup>6</sup>Department of Obstetrics, Leiden University Medical Center, Leiden, the Netherlands.

*\*These authors contributed equally to this work*



## Abstract

Most studies on growth plate (GP) maturation and fusion have been carried out in animal models not fully representing the human epiphyseal GP. We used human fetal bone marrow-derived mesenchymal stem cells (hfMSCs) differentiating towards chondrocytes as an alternative model for the GP. Our aims were to assess whether chondrocytes derived from hfMSCs are a valid model for the GP and to study gene expression patterns associated with chondrogenic differentiation.

Microarray and principal component analysis were applied to study gene expression profiles during chondrogenic differentiation. A set of 315 genes was found to correlate with *in vitro* cartilage formation. Several identified genes are known to be involved in cartilage formation and validate the robustness of the differentiating hfMSC model. Other genes like Bradykinin and IFN- $\gamma$  signaling, CCL20, and KIT were not described in association with chondrogenesis before. KEGG pathway analysis using the 315 genes revealed 9 significant signaling pathways correlated with cartilage formation.

To determine which type of hyaline cartilage is formed, we compared the gene expression profile of differentiating hfMSCs with previously established expression profiles of human articular (AC) and epiphyseal GP cartilage. As differentiation towards chondrocytes proceeds, hfMSCs gradually obtain a gene expression profile similar to epiphyseal GP cartilage, but less resembling the fingerprint of AC. This study validates differentiating bone marrow-derived hfMSCs as an excellent model for the epiphyseal GP. The hfMSC model offers the opportunity to unravel molecular mechanisms underlying growth regulation as they occur in the human growth plate.

## Introduction

Growth of the long bones of the human skeleton occurs as the result of a tightly orchestrated proliferation and differentiation program called endochondral ossification. In the epiphyseal growth plate of long bones, chondrocytes originating from mesenchymal stem cells subsequently undergo proliferation, hypertrophic differentiation, and programmed cell death before being replaced by bone. At the time of sexual maturation, growth first increases but at the end of puberty epiphyseal fusion and termination of growth occur. Our knowledge on the molecular mechanisms underlying growth regulation is limited, although estrogen has been identified as a key regulator of growth plate maturation and fusion (1). Gaining a detailed understanding of growth regulatory processes is essential to facilitate the development of novel strategies for the treatment of various growth disorders.

Commonly used animal models for studying growth plate regulation do not fully represent the human epiphyseal plate. For example, rodent growth plates do not fuse at the end of sexual maturation (2), and therefore do not display an important hallmark of human growth plate development. The shortcoming of the mouse model is clearly demonstrated by the contrast between the marginally affected growth phenotype of the estrogen receptor alpha (ER $\alpha$ ) knock out mouse ( $\alpha$ ERKO) (3) and the prominent growth phenotype of a male patient lacking functional ER $\alpha$  (4), characterized by the absence of epiphyseal fusion and continuation of growth into adulthood. The lack of representative animal models has led to the realization that alternative human models are essential to elucidate the mechanisms involved in growth plate regulation and fusion. However, human growth plate specimens are difficult to obtain, whereas *in vitro* models such as chondrosarcoma cell lines or articular cartilage-derived chondrocyte cultures have limited differentiation capacity, are often difficult to maintain under laboratory conditions or

tend to dedifferentiate. Furthermore, articular cartilage and growth plate cartilage have distinct functions and it is therefore questionable whether articular cartilage-derived chondrocytes are representative for epiphyseal growth plate chondrocytes.

Multipotent human mesenchymal stem cells (hMSCs) are a promising *in vitro* model to study chondrogenesis. They have been postulated as an alternative cell source for articular cartilage reconstruction and for studying endochondral ossification as it occurs in the epiphyseal growth plate (5). In this study, we explored the cartilage forming capacity of human fetal (hf)MSCs to create an *in vitro* model for the human growth plate. We have chosen human fetal bone marrow-derived MSC for their superior differentiation characteristics compared to adult bone marrow-derived MSCs (6). Efficient cartilage formation was demonstrated by immunohistochemical analysis and gene expression profiling was applied to identify genetic pathways involved in the differentiation process. In addition, the gene expression profiles of the differentiating hfMSCs were compared with global gene expression patterns of human articular and growth plate cartilage to assess whether differentiating hfMSCs represent either articular or growth plate chondrocytes.

## **Materials and methods**

### **Cell culture**

The use of human fetal material was approved by the medical ethical committee of the Leiden University Medical Center and an informed consent was obtained from the women undergoing elective abortion. Cell suspensions of fetal bone marrow were obtained by flushing the long bones of fetuses with M199 washing medium. For the chondrogenic differentiation and microarray analysis, cells derived from a single 22 weeks old fetus were used. MSCs derived from other fetuses were also stimulated to undergo chondrogenic differentiation. Red cells were depleted by incubation for 10 minutes in  $\text{NH}_4\text{Cl}$  (8.4 g/L)/ $\text{KHCO}_3$  (1g /L) buffer at 4°C. Mononuclear cells were plated at a density of  $16 \times 10^4$  cells/cm<sup>2</sup> in M199 culture medium (Gibco) supplemented with 10% fetal bovine serum (FBS), 1% penicillin/streptavidin (P/S), fungizone, endothelial cell growth factor (ECGF) 20 µg/ml (Roche Diagnostics) and heparin 8 U/ml in culture flasks (Greiner) coated with 1% gelatin. Cultures were kept in a humidified atmosphere at 37°C with 5% CO<sub>2</sub>. The culture medium was changed twice per week. After reaching near-confluence at passage 4 to 5, hfMSCs were harvested by treatment with 0.5 % trypsin and 0.5% ethylene diamine tetra acetic acid (EDTA; Gibco) for 5 minutes at 37°C and replated for chondrogenic differentiation.

### **In vitro chondrogenic differentiation**

hfMSCs ( $2 \times 10^5$  cells/well) were positioned into pellets by centrifugation at 1200 rpm for 4 minutes in U-shaped 96-well suspension culture plates (Greiner) and cultured at 37°C with 5% CO<sub>2</sub> in 200 µl of serum-free chondrogenic medium consisting of high-glucose (25 mM) Dulbecco's modified Eagle's medium (DMEM; Gibco) supplemented with 40 µg/ml proline (Sigma), 100 µg/ml sodium pyruvate (Sigma, USA), 50 mg/ml ITS (insulin-transferrin-selenic acid) with Premix (BD Biosciences), 1% Glutamax (Gibco), 1% penicillin/streptavidin, 50 g/ml ascorbate-2-phosphate (Sigma),  $10^{-7}$  M dexamethasone (Sigma), 10 ng/ml transforming growth factor-β3 (TGF-β3; R&D Systems), 500 ng/ml bone morphogenetic protein 6 (BMP6) and antibiotic and antimycotic mix (0.06% polymixin, 0.2% kanamycin, 0.2% penicillin, 0.2% streptavidin, 0.02% nystatin and 0.5% amphotericin. The medium was changed twice per week for 5 weeks.

### ***Histological analysis***

Two pellets per time point (after 1, 2, 3, 4, or 5 weeks of chondrogenesis) were used for histological evaluation. Pellets were fixed in 10% formalin, dehydrated by treatment with graded ethanols and processed for paraffin embedding. 5  $\mu$ m sections were cut using a Reichert Jung 2055 microtome (Leica). For each pellet, only the sections from exactly the center of the pellets were mounted on glass slides. Before histological (toluidine blue) or immunohistochemical staining, sections were deparaffinized in xylene and graded ethanols followed by three washing steps phosphate buffered saline (PBS).

For immunohistochemistry, sections were preincubated with blocking buffer (1% H<sub>2</sub>O<sub>2</sub> in 40% methanol, 60% tris buffered saline) twice for 15 minutes at room temperature, followed by overnight incubation at 4°C with mouse monoclonal antibody against collagen type II or type X in a 1:100 dilution (Quartett). Next, sections were incubated with the secondary antibody biotinylated rabbit-anti-mouse IgG (DAKO) in a 1:300 dilution, followed by incubation with horseradish-peroxidase-conjugated-streptavidine (Amersham Biosciences). Staining was visualized with 3-amino-9-ethylcarbazole substrate in 0.2 mg/ml acetate buffer (pH 5.2) with 0.04% H<sub>2</sub>O<sub>2</sub>. After counterstaining with hematoxylin, the sections were mounted in Histomount (National Diagnostics). Pictures of the stained pellets were taken with a Nikon DXM 1200 digital camera using standardized settings.

### ***RNA isolation***

Total RNA from 2·10<sup>6</sup> undifferentiated hMSCs derived from the 22-weeks old fetus was extracted with Trizol (Invitrogen). After 1, 2, 3, 4, or 5 weeks of chondrogenesis, 60 pellets (per time point) were pooled and homogenized in 1ml 4M guanidine isothiocyanate solution (Sigma) and RNA was extracted according to the optimized method for RNA extraction from cartilage as described by Heinrichs et al. (43). The extracted total RNA was purified using the RNeasy kit according to recommendations of the manufacturer (Qiagen).

### ***Gene expression profiling***

High RNA quality was confirmed by capillary electrophoresis on an Agilent 2100 bioanalyzer (Agilent). Total RNA (100 ng) was amplified and labeled using the GeneChip Two-Cycle cDNA Synthesis Kit (Affymetrix) and the MEGAscript T7 Kit (Ambion). For gene expression profiling, labeled cRNA was hybridized in duplicate to Affymetrix Human Genome U133 PLUS 2.0 Array Genechips. All procedures were carried out according to the manufacturer's recommendations.

Raw data from Affymetrix CEL files were analyzed using SAS software package Microarray Solution version 1.3 (SAS Institute). Custom CDF version 10 with Entrez based gene definitions (44) was applied to map the probes to genes. Gene annotation was obtained using the Affymetrix NetAffx website (<http://www.affymetrix.com/analysis/index.affx>). Quality control, normalization and statistical modeling were performed by array group correlation, mixed model normalization and mixed model analysis respectively. The normalized expression values for each gene were standardized by linearly scaling the values across all samples of the time course to a mean of 0 with an SD of 1. Analysis of differential gene expression was based on loglinear mixed model of perfect matches (45). A false discovery rate of  $\alpha=0.05$  with Bonferroni-correction for multiple testing was used to set the level of significance. The raw and normalized data are deposited in the Gene Expression Omnibus database (<http://www.ncbi.nlm.nih.gov/geo/>; accession no. GSE-XXXX).

### ***Microarray data analysis***

The statistical analysis of the microarray data was based on the normalized mean expression values per probe at 6 time points with 2 replications at each time point (12 observations per probe).

In order to identify subgroups of probes with similar expression profiles over time, a principal component analysis (PCA) of the covariance matrix was carried out on the mean expression value for each probe at each time point. For each probe, factor scores for principal components 1, 2 and 3 were obtained by regression analysis of the 12 array results (6 time points in duplicate) for that specific probe to those components. The first principal component corresponded with the general expression level during the whole experiment, whereas the second and third component corresponded with changes over time. Since our interest was to identify genes associated with the changes that occur during differentiation from stem cells towards chondrocytes, we focused our analysis on the second and third component. By construction, these factor scores had a mean of 0 with an SD of 1. Generally, the distribution over the factor scores showed a normal distribution with outliers. We used a cut-off of  $\pm 3.29$  to select outlying probes. This cut-off would select 0.1% of the probes, if the factors scores would follow a pure normal distribution that could be expected if the data were pure noise. The presence of replications allowed us to assess the statistical significance of the factor scores and to remove probes that were not significant at the  $\alpha=5\%$  level. In a separate study we compared the gene expression profiles of human articular cartilage (AC) and epiphyseal growth plate (GP) cartilage. A set of 1818 significant differentially expressed genes was identified, that can be used to discriminate between the two hyaline cartilage subtypes (Leijten et al., manuscript in preparation). All AC (n=5) and GP (n=5) samples were derived from 9 to 17 year old female donors with no history of growth disorders. The gene expression profiles of the stem cells differentiating towards chondrocytes were compared with this list. Principal component analysis (PCA) with Pearson product-moment correlation was performed to compute correlations between the expression profiles.

### ***Pathway analysis***

Using sets of probes emerging from PCA, a search for relevant KEGG pathways was performed using the DAVID® Knowledgebase, a publicly available bioinformatics tool for functional annotation (<http://david.abcc.ncifcrf.gov>).

### ***Quantitative real-time polymerase chain reaction (qPCR)***

RNA was transcribed into cDNA using the First Strand cDNA Synthesis kit for qPCR (Roche Diagnostics) according to the manufacturer's protocol. Specific primer sets (available on request) were designed to amplify aggrecan (ACAN), pannexin 3 (PANX3), epiphygan (EPYC), collagen type II (COL2), and type X (COL10), SRY-box 9 (SOX9), WNT11, lymphoid enhancer-binding factor 1 (LEF1), Gremlin 1 (GREM1), and the housekeeping genes  $\beta_2$ -microglobulin, and glyceraldehyde 3-phosphate dehydrogenase (GAPDH). In order to test donor inter-variation, differentiated MSCs isolated from other fetal donors were used for qPCR analysis as well.

All PCR reactions were performed in triplicate with 5 ng cDNA and according to the manufacturer's protocol of the iQ™ SYBR® Green Kit (Biorad) in a final volume of 25  $\mu$ l. The cDNA was amplified using the following thermal cycling conditions: one cycle at 50°C for 2 min and 95°C for 10 min, followed by 40 cycles of 15 s at 95°C and 1 min at 56°C. Fluorescence spectra were recorded and the threshold cycle number (Ct) was read. For each time point mean Ct was calculated and from this value the fold difference in expression between undifferentiated hfMSCs and differentiating cells according to the equation  $2^{-\Delta\Delta Ct}$  (normalized fold expression). For visualization, this value was log-transformed.



# Results

## Chondrogenic differentiation by hfMSCs

### Evaluation of protein and mRNA expression

Immunohistological evaluation showed an increasing expression of cartilage markers with time and a gradual morphological change from stem cells to mature and hypertrophic chondrocytes (figure 1). The mean diameter of the pellets increased with time, as well as the amount of glycosaminoglycans, a major constituent of the cartilaginous extracellular matrix. Immunohistochemical staining for collagen type II demonstrated the presence of chondrocytes after 1 week of pellet culture. Hypertrophic chondrocytes were first detected after 3 weeks, as detected by immunohistochemical staining for collagen type X. At the last stage of differentiation, the pellets display a two-layered structure with a core that consists of chondrocytes and that is surrounded by a thin outer layer of undifferentiated thin spindle-shaped cells.

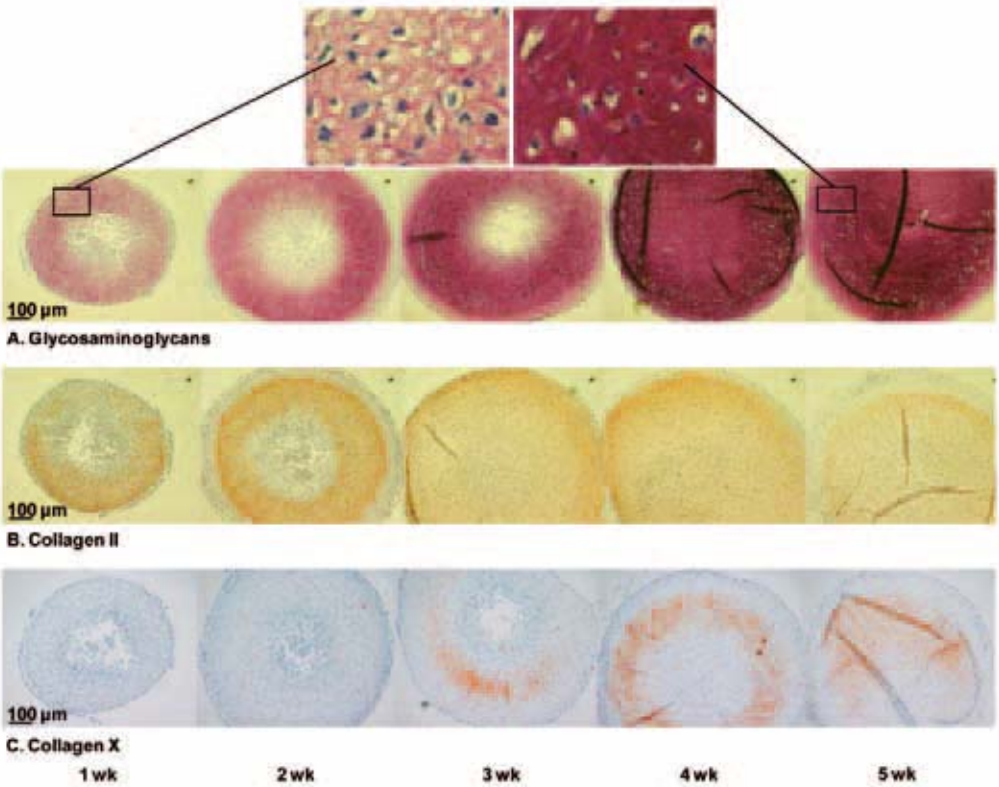


Figure 1

Expression of (A) glycosaminoglycans visualized by toluidine blue staining, (B) collagen type II immunohistochemistry (brown), and (C) collagen type X immunohistochemistry (brown) during 5 weeks of chondrogenic differentiation of hfMSCs to chondrocytes.

From each time point RNA was isolated and subjected to microarray analysis. Changes in gene expression of a subset of genes consisting of both established marker genes for chondrogenesis and differentially expressed genes identified by microarray analysis were validated using qPCR (figure 2). In concordance with the observations of immunohistological markers of chondrogenesis, microarray data and qPCR showed time-dependent increases in the expression of the cartilage markers collagen type II, and type X, SOX9, and aggrecan mRNA. To further extend this analysis, we randomly selected 7 genes (pannexin 3, epiphygan, WNT11, LEF1, gremlin 1, Dickkopf 1, matrilin) that showed marked regulation over time based on microarray analysis. Again, qPCR demonstrated a strong correlation between the expression patterns revealed by both techniques (results for 5 of these genes are shown in figure 2E-I), providing further support for the robustness of our dataset. Repeating the qPCR analysis using RNA isolated from other fetal donors of MSCs that were stimulated to undergo chondrogenic differentiation rendered similar gene expression patterns as observed for the single 22-weeks old donor derived cells (data not shown).

### ***Principal component analysis and KEGG pathway analysis***

The sequential changes that occur during chondrogenic differentiation in the hfMSC model were studied with bioinformatics analysis of the microarray data. Using principal component analysis, three components were found to explain 99.6% of the variance within our dataset (figure 3.A). The factor loadings in figure 3.B show that component 1 describes a general level of gene expression, as expected. Component 2 shows to what extent gene expression changed with time during chondrogenic differentiation and component 3 signifies whether there was an additional, short term elevation or dip in expression around 2 to 3 weeks of differentiation. Since components 2 and 3 were most likely to contain genes associated with the loss of stem cell characteristics or the gain of a chondrocyte phenotype, we focused on those components.

Using the  $\pm 3.29$  cut-off in combination with a 5% significance test, we distinguished four subgroups of probes. The precise definitions and the resulting numbers of these subgroups are given in figure 3.C. The scatter plot in figure 3.D illustrates that the numbers of probes in subgroups 1 and 2 are much larger than the 9 probes (0.05%) that would have been expected under purely random selection. Moreover, in these two subgroups nearly all probes in the first selection are significant at the 5% level, suggesting that the number of false discoveries in these two groups is quite small. More noise is presumably present in the smaller subgroups 3 and 4 based on factor 3 scores.

The profiles of the selected probes demonstrate that subgroup 1 containing the largest number of probes ( $n=146$ ) describes a peak of expression on  $t_0$  followed by a decrease in expression thereafter. In contrast, the second largest subgroup of probes ( $n=105$ ) in profile 2 demonstrates increasing expression levels from  $t_0$  onward. The smaller subgroups 3 and 4 demonstrate lower levels of expression with profile 3 ( $n=49$ ) showing a short-term increase in expression at  $t_1$  followed by decreases thereafter and profile 4 ( $n= 15$ ) displaying a short-term expression dip between  $t_1$ - $t_2$ .

A total of 83 out of 315 probes could not be annotated and was discarded from further analysis. The remaining 232 probes that could be matched to genes (supplementary table 1) were used to identify 9 KEGG pathways that were significantly associated with chondrogenic differentiation and contained 39 genes. (figure 4). Some genes were present solely in one pathway ( $n= 23$ ), but others were found in 2 ( $n= 6$ ) or 3 ( $n= 10$ ) pathways (table 1). Three functional groups of genes were recognized: 1) growth factor (GF) and GF-related genes; 2) genes associated with the extracellular matrix; and 3) genes associated with signal transduction, cell cycle, and cell survival.

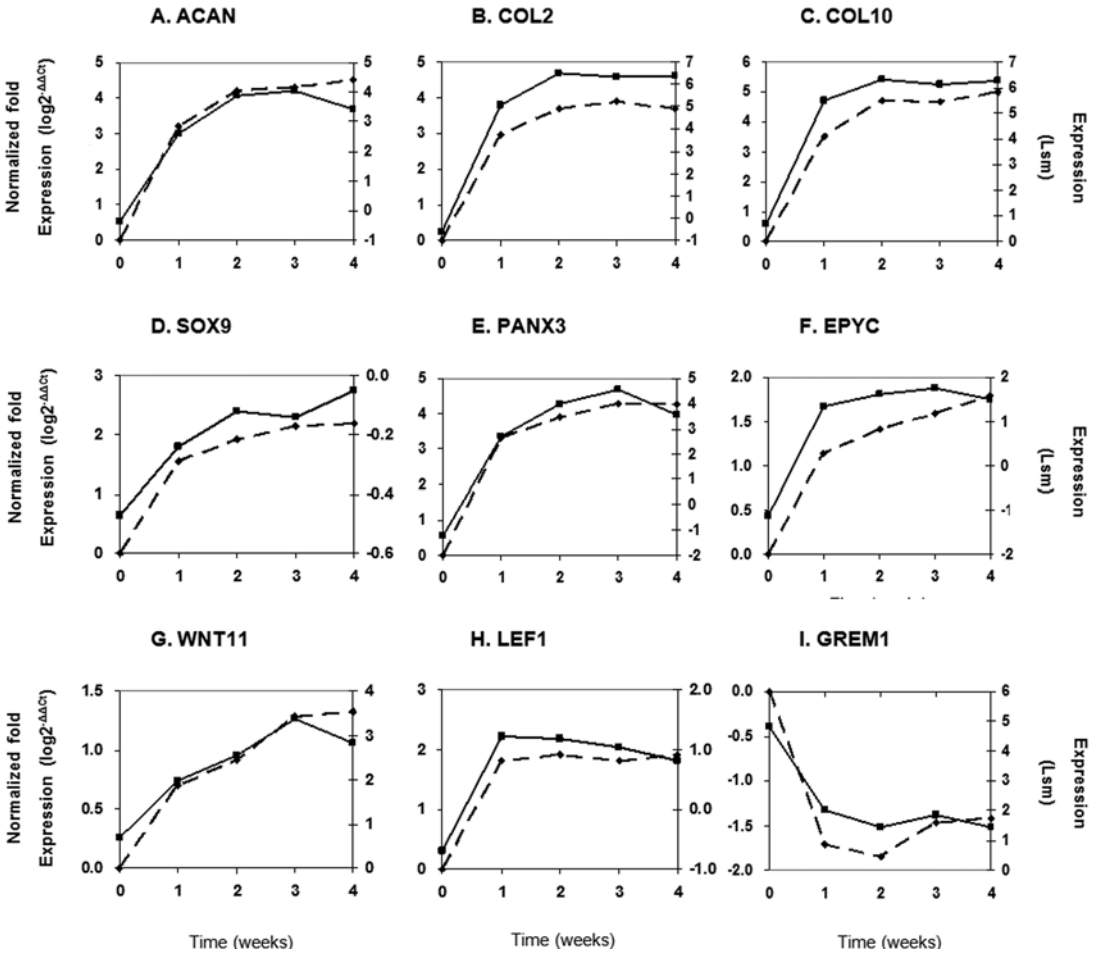


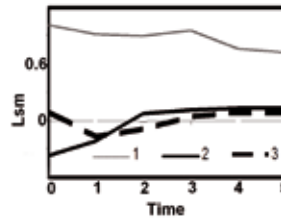
Figure 2

Correlation between qPCR and microarray expression data for (A) aggrecan, (B) collagen II, (C) collagen X, (D) SOX9, (E) pannexin 3, (F) epiphycan, (G) WNT11, (H) LEF1, and (I) gremlin 1 during 5 weeks of chondrogenic differentiation of hMSCs. qPCR data are expressed as delta delta CT values corrected for the housekeeping gene  $\beta 2$ -microglobulin. The primary y-axis (left) indicates the qPCR results as normalized fold expression on a log-scale. The secondary y-axis (right) indicates the microarray analysis results as least square means (Lsm).

A. Variance explained by PCA

Component	Variance (%)	Cumulative variance (%)
1	95.16	95.16
2	3.24	98.40
3	1.15	99.55
4+5+6	0.45	100

B. Principal components



C. Subgroup definitions

Subgroup	Factor 2 score	Factor 3 score	Nº. of probes	Sign. probes
1	$\leq -3.29$		149	146
2	$\geq 3.29$		118	105
3	$< -3.29$	$\leq -3.29$	135	49
4	$> 3.29$	$\geq -3.29$	64	15

D. Expression profiles

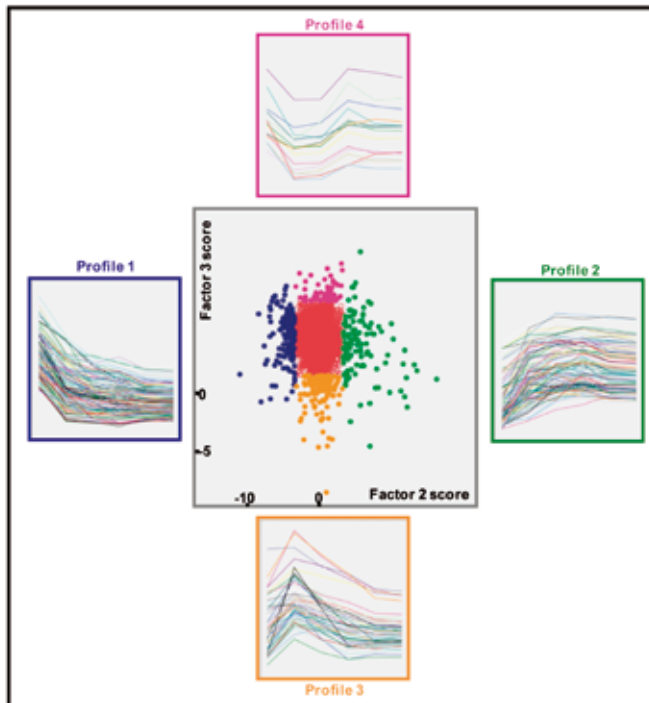


Figure 3

Gene selection based on principal component analysis. A) variance explained by components 1-6 from principal component analysis. B) principal components 1, 2, and 3 as expression profiles. C) selection of probes based on their factor 2 and 3 scores. D) scatterplot view of gene data in respect to their correlation (factor score) to principal components 2 and 3. Subgroups 1, 2, 3, and 4 are represented by blue, green, yellow, and pink dots, respectively. Side-placed graphs depict the gene expression profiles for genes found in the four subgroups.

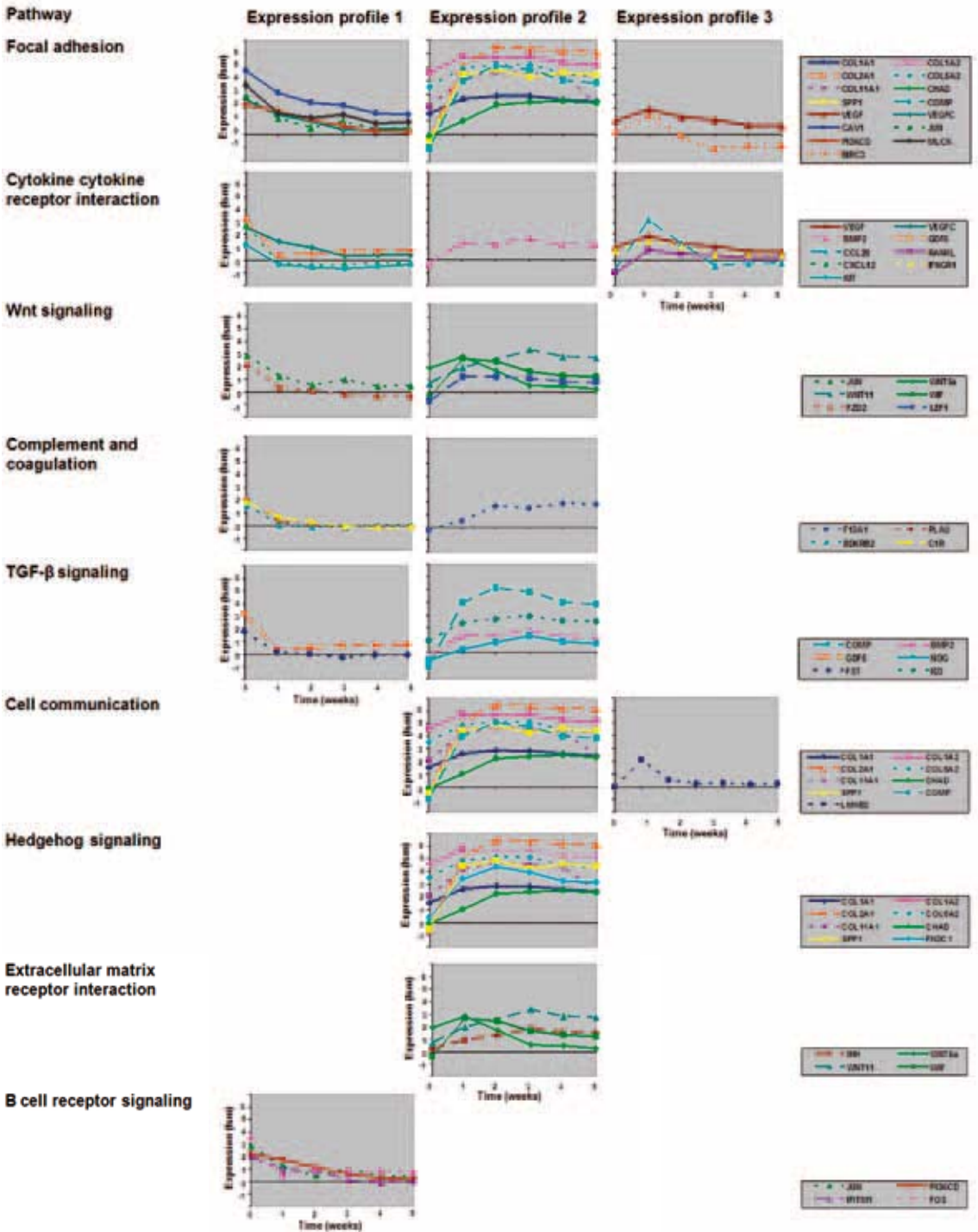


Figure 4

KEGG signaling pathways significantly associated with chondrogenic differentiation of hMSCs. For each pathway, genes showing the same distinct expression profile during 5 weeks of chondrogenic differentiation are depicted as groups.

### Gene expression fingerprinting for cartilage subtype

Histological and gene expression analyses showed that the differentiating hfMSCs acquire a hyaline cartilage phenotype. Two major types of hyaline cartilage can be distinguished, namely articular and epiphyseal cartilage. In order to serve as a model for the epiphyseal growth plate, differentiating hfMSCs should obtain a growth plate signature. To test this, we compared the expression profiles of the differentiating hfMSCs with previously established profiles of human articular and growth plate cartilage (AC and GP, respectively, Leijten et al., in preparation). In a three-dimensional schematic representation, samples of AC and GP plot in two different groups (figure 5). As expected, AC, GP, and undifferentiated hfMSCs (hMSC\_t0) plotted as distinct entities in a three-dimensional space. As differentiation progressed, the expression profile of the hfMSCs changed, and the differentiating chondrocytes gradually acquired a fingerprint resembling GP, but not AC. This analysis demonstrated that the hfMSCs differentiating towards chondrocytes acquired a GP cartilage phenotype.

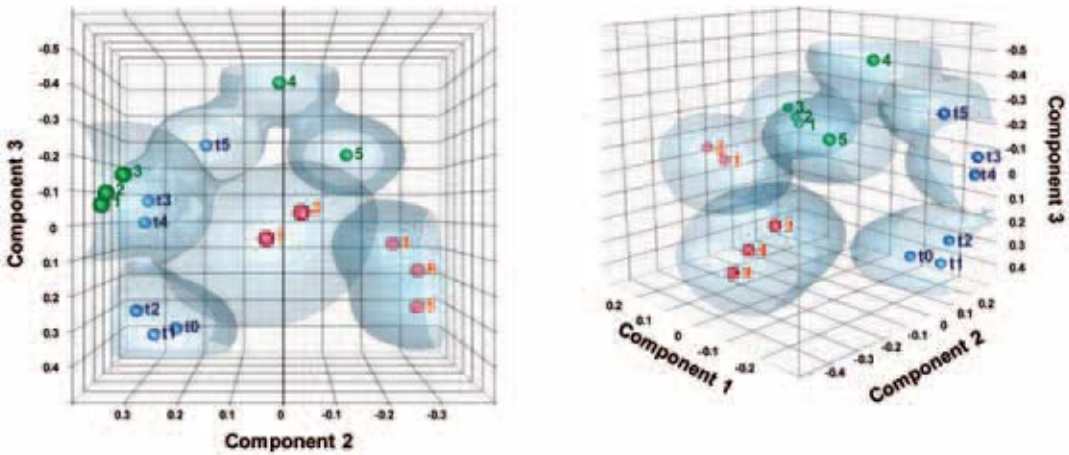


Figure 5

Three-dimensional overviews of gene expression data in respect to their correlation (factor score) to principal components 1, 2, and 3. Red dots, samples of articular cartilage; Green dots, samples of growth plates; Blue dots, differentiation time-range of hfMSCs (t0, undifferentiated hfMSCs; t5, mature chondrocytes). Dots indicate the mean factor score for all genes on the Affymetrix chip on the three principal components for one cartilage sample. Clouds represent the spread around the mean factor score in three dimensions.

## Discussion

The present study was conducted in order to determine whether fetal bone marrow-derived MSCs are a representative human model for studying processes taking place in the epiphyseal growth plate and to identify associated signaling pathways. It has been reported that human bone marrow-derived MSCs display a better chondrogenic differentiation capacity than those derived from other sources, with fetal being superior over adult MSCs (6). Consequently, it seems appropriate to use fetal bone marrow-derived MSCs as a model for chondrogenesis. However, fetal MSCs are not easily obtained, due to ethical and legal considerations, and as a consequence, adult bone marrow-derived MSCs have been used in many previous studies (7-14).

Chondrogenic differentiation occurred in our *in vitro* model, as illustrated by the progressive expression of the chondrocyte markers collagen type II and X and the cartilaginous matrix constituent glycosaminoglycan. The two-layered structure that developed in the pellet during chondrogenic differentiation indicates that the differentiation was more successful in the core of the pellet.

Further confirmation of chondrogenesis was obtained by analysis of mRNA expression of cartilage markers, which, in addition, also validated our microarray results. The observation of similar gene expression patterns for all analyzed markers during chondrogenic development of MSCs derived from other fetal donors indicates that the selected 22-weeks old fetal MSC-donor was representative for fetal bone marrow in general.

Matrix mineralization was not observed after 5 weeks of differentiation, suggesting that the matrix was not ready for mineralization or that environmental stimuli necessary to induce this process were absent.

Microarray analysis generated a multidimensional dataset of differentially expressed genes for each time point. Several methods for analyzing such complex data have been reported, many based on presence/absence analysis, which starts with the list of differentially expressed genes and applies a strict but arbitrary cut-off for differential expression of individual genes (9;14). Misinterpretation of the data can easily occur, since genes are assumed to be independent, whereas it is more likely that sets of correlated genes play a role in complex biological processes (15). Genes that are not considered differentially expressed, but that do play a role in important signaling pathways, may be wrongfully eliminated. Another analysis strategy applied by many groups is to report on *a priori* selected pathway(s) of interest, thereby disregarding the relative importance of this pathway in view of other potentially co-regulated or interacting pathways. Alternatively, we have applied PCA with restrictive criteria as a statistical selection method for identification of gene expression profiles associated with the acquisition of chondrocyte characteristics or the loss of a stem cell phenotype. Since biological replicates were not included in this study, such a stringent approach was necessary in order to minimize potentially false-positive results.

The gene expression data generated with this analytic approach are consistent with previous reports on *in vitro* cartilage formation by adult mesenchymal stem cells. We therefore conclude that PCA is a suitable and unbiased analysis tool for data reduction in multidimensional and complex microarray experiments. Using this method, 232 genes were identified to be significantly associated with chondrogenic differentiation, 39 of which were present in 9 significantly enriched KEGG pathways. These 39 genes could be classified in three major functional groups that are discussed in the following sections.

### **Growth factor (GF) and GF-related genes**

Growth factors from the transforming growth factor  $\beta$  (TGF- $\beta$ ), Wnt, Hedgehog and VEGF families have been recognized as major regulators of endochondral bone formation in embryonic and postnatal cartilage development (16;17). Some family members were also identified to be involved in chondrocyte differentiation in our *in vitro* model.

BMP2 and its downstream effector ID3 are upregulated early in differentiation consistent with previous reports on the importance of BMP signaling in chondrogenesis (18;19). Growth and differentiation factor 5 (GDF5), previously reported as stimulator of chondrocyte proliferation (20), was highly expressed at the earliest time point observed and downregulated thereafter. A similar expression profile was found for the BMP inhibitor follistatin (FST) that was previously shown to be expressed by proliferative, but not by hypertrophic chondrocytes (21).

Previous *in vitro* studies have demonstrated that BMP2 interacts with Wnt and hedgehog family members and their downstream effectors, indicating that functional crosstalk between regulatory pathways occurs during chondrogenesis (19;22). Such interactions may have taken place in our *in vitro* model as well since several genes out of the Wnt and Hedgehog family were affected during differentiation, e.g. WNT5a, WNT11, FZD2, WIF1 and IHH. IHH expression reached a maximum after 3 weeks of differentiation, which is in agreement with a stimulatory, PTHrP-independent effect of IHH on terminal chondrocyte differentiation in the postnatal growth plate.

Another major group of regulatory factors found to be involved in chondrogenesis was the superfamily of cytokines. Several genes in this group were changing significantly over time, e.g. CXCL12, CCL20, interferon- $\gamma$  (IFN- $\gamma$ ), IFN- $\gamma$  receptor IFNGR1, interferon-induced transmembrane protein 1 (IFITM1) and the cytokine RANKL (receptor activator for nuclear factor  $\kappa$  B ligand). To our knowledge a role for CCL20, IFITM1, IFN- $\gamma$  and its receptor IFNGR1 has not been described before in chondrogenesis.

Vascular endothelial growth factors (VEGF and VEGFC), originally described to promote epiphyseal vascularization prior to endochondral ossification, also regulate *in vitro* chondrogenesis (23-25). Both VEGF and VEGFC were significantly changing in expression level early in our model.

### **Genes associated with the extracellular matrix**

Progression of chondrogenic differentiation depends on the coordinated expression of ECM components and on cell-matrix interactions (16). Several genes involved in focal adhesion, cell-matrix communication, ECM receptor interaction and matrix remodeling were found to play a role in our *in vitro* model of chondrogenesis.

The expression of cartilaginous ECM proteins, such as collagens (COL1A1, COL1A2, COL2A1, COL5A2, COL11A1), chondroadherin (CHAD), cartilage oligomeric matrix protein (COMP), secreted phosphoprotein 1 (osteopontin, SPP1), and fibronectin type III (FNDC1), was upregulated. Apart from a structural role in the extracellular matrix, FNDC1, SPP1 and CHAD also function as integrin ligands and regulate cell-matrix signaling by binding to the cell surface plasma membrane protein integrinT. Aggregation of integrins in focal adhesions is induced by activity of myosin light chain kinase (MLCK) (26). Upon ligand-integrin binding, signaling complexes are activated that mediate downstream effectors of integrin signaling such as phosphoinositide-3-kinase (PI3K) (27), thereby stimulating cell proliferation (28). We observed early downregulation of integrin signaling-related proteins such as PI3K and MLCK.

Members of the complement and coagulation family of proteins were expressed during *in vitro* chondrogenic differentiation. Coagulation factor XIII (F13A1) expression was upregulated, other genes like complement component I (C1R), urokinase-type plasminogen activator (PLAU) and bradykinin receptor B2 (BDKRB2) were downregulated during differentiation in our model. These



proteins are associated with matrix mineralization (29-31) or matrix degradation in the growth plate (32-34).

### ***Genes associated with signal transduction, cell cycle, and cell survival***

Several genes involved in the regulation of cell survival and proliferation and signal transduction were found to be important in our *in vitro* model of chondrogenesis. Caveolin 1 (CAV1), a multifunctional scaffolding protein located at cell surface caveolae, regulates TGF, Wnt, cytokine and VEGF signaling by modulating their downstream signaling cascades such as JAK/STAT,  $\beta$ -catenin/LEF1, MAPK/ERK and PI3K/AKT (35-38). The anti-apoptotic baculoviral IAP repeat containing 3 (BIRC3) has been shown to increase the survival of cultured human chondrocytes (39). Phosphoinositide-3-kinase (PI3K), proto-oncogene KIT, transcription factor JUN and FOS are all associated to the regulation of cell proliferation (40; 41). Expression of the nuclear envelope protein lamin B2 (LMNB2) was first upregulated and later in differentiation downregulated in our model. Constantinescu et al suggested a role for LMNB2 in suppressing differentiation of undifferentiated embryonic stem cells (42).

### ***Conclusion***

Many genes identified in this study were previously reported in association with chondrogenesis, validating the robustness of differentiating hfMSC as a model for cartilage formation. The implication of bradykinin and IFN- $\gamma$  signaling, CCL20, and KIT are novel findings. Discrepancies between our results and reports by others may rely on differences between the source, and chondrogenic capacity of MSCs used, the experimental conditions for inducing chondrogenesis, and the gene expression analysis methods (9;10;13). Developmental genes essential for chondrogenic differentiation (e.g. SOX genes, IGF-I) were not identified, in line with other reports (11). Marginal changes in the expression of these genes may be sufficient for inducing major effects, but too subtle to be detected by most gene expression analysis methods, including PCA. Alternatively, changes occurring within the first days of differentiation may have been unnoticed due to the chosen time interval of analysis.

This study has demonstrated for the first time that bone marrow-derived hfMSCs acquire a GP-, but less an AC-like signature during differentiation towards chondrocytes. These findings validate differentiating hfMSCs as an excellent model for the epiphyseal growth plate. The application of this model in future studies creates the opportunity to unravel molecular mechanisms underlying growth regulation in the human epiphyseal plate and allows the analysis of even the earliest stages of chondrogenic differentiation. The effects of specific signaling pathways and growth-associated hormones (e.g. estrogen), can be studied and (genetically) manipulated in this model, which may give an impulse to the development of novel treatment strategies in various growth disorders.

## ***Acknowledgement and funding***

This work was supported by a grant from the European Society for Paediatric Endocrinology Research Unit and by grants from ZonMW, the Netherlands Organisation for Health Research and Development, to S.A. van Gool (grant number 920-03-392) and J.A.M. Emons (grant number 920-03-358) and a grant from the Deutsche Forschungsgemeinschaft to G.Rappold (Ra380/12-1). The authors gratefully acknowledge the TeRM Smart Mix Program of the Netherlands Ministry of Economic Affairs and the Netherlands Ministry of Education, Culture and Science.

## Supplemental table 1

Affymetrix ID	Gene code	Gene title
205856_at	SLC14A1	solute carrier family 14 (urea transporter), member 1 (Kidd blood group)
205911_at	PTHRI	parathyroid hormone receptor 1
219148_at	PBK	PDZ binding kinase
213182_x_at	CDKN1C	cyclin-dependent kinase inhibitor 1C (p57, Kip2)
206737_at	WNT11	wingless-type MMTV integration site family, member 11
203868_s_at	VCAM1	vascular cell adhesion molecule 1
218730_s_at	OGN	osteolectin (osteoinductive factor, mimecan)
200665_s_at	SPARC	secreted protein, acidic, cysteine-rich (osteonectin)
223484_at	C15orf48	chromosome 15 open reading frame 48
206315_at	CRLF1	cytokine receptor-like factor 1
205497_at	ZNF175	zinc finger protein 175
204724_s_at	COL9A3	collagen, type IX, alpha 3
219410_at	TMEM45A	transmembrane protein 45A
218391_at	SNF8	SNF8, ESCRT-II complex subunit, homolog (S. cerevisiae)
210538_s_at	BIRC3	baculoviral IAP repeat-containing 3
201487_at	CTSC	cathepsin C
219134_at	ELTD1	EGF, latrophilin and seven transmembrane domain containing 1
212551_at	CAP2	CAP, adenylate cyclase-associated protein, 2 (yeast)
206421_s_at	SERPINF7	serpin peptidase inhibitor, clade B (ovalbumin), member 7
219837_s_at	CYTL1	cytokine-like 1
210220_at	FZD2	frizzled homolog 2 (Drosophila)
207064_s_at	AOC2	amine oxidase, copper containing 2 (retina-specific)
218542_at	CEP55	centrosomal protein 55kDa
206423_at	ANGPTL7	angiopoietin-like 7
231227_at	---	Transcribed locus, strongly similar to WNT-5A protein precursor
229494_s_at	CD63	CD63 molecule
223734_at	OSAP	ovary-specific acidic protein
206614_at	GDF5	growth differentiation factor 5 (cartilage-derived morphogenetic protein-1)
205713_s_at	COMP	cartilage oligomeric matrix protein
230372_at	---	Transcribed locus, PREDICTED: similar to hyaluronan synthase 2 [Pan troglodytes]
1563724_at	SACS	Spastic ataxia of Charlevoix-Saguenay (sacsin)
203499_at	EPHA2	EPH receptor A2
1556499_s_at	COL1A1	collagen, type I, alpha 1
219230_at	TMEM100	transmembrane protein 100
206790_s_at	NDUFB1	NADH dehydrogenase (ubiquinone) 1 beta subcomplex, 1, 7kDa
204825_at	MELK	maternal embryonic leucine zipper kinase
212565_at	STK38L	serine/threonine kinase 38 like
1554997_a_at	PTGS2	prostaglandin-endoperoxide synthase 2 (prostaglandin G/H synthase & cyclooxygenase)
204894_s_at	AOC3	amine oxidase, copper containing 3 (vascular adhesion protein 1)
203886_s_at	FBLN2	fibulin 2
203153_at	IFIT1	interferon-induced protein with tetratricopeptide repeats 1
242517_at	KISS1R	KISS1 receptor
1552340_at	SP7	Sp7 transcription factor
203963_at	CA12	carbonic anhydrase XII
1554950_at	AGC1	aggrecan 1 (chondroitin sulfate proteoglycan 1, large aggregating proteoglycan)
232451_at	---	MRNA; cDNA DKFZp564I0816 (from clone DKFZp564I0816)
227705_at	TCEAL7	transcription elongation factor A (SII)-like 7
1570574_at	GPR177	G protein-coupled receptor 177
218273_s_at	PPM2C	protein phosphatase 2C, magnesium-dependent, catalytic subunit
224735_at	CYBASC3	cytochrome b, ascorbate dependent 3
239787_at	KCTD4	potassium channel tetramerisation domain containing 4
226281_at	DNER	delta-notch-like EGF repeat-containing transmembrane
218839_at	HEY1	hair/enhancer-of-split related with YRPW motif 1
214710_s_at	CCNB1	cyclin B1
231798_at	NOG	Noggin
204595_s_at	STC1	stanniocalcin 1
209189_at	FOS	v-fos FBJ murine osteosarcoma viral oncogene homolog
203297_s_at	JARID2	Jumonji, AT rich interactive domain 2
230137_at	TMEM155	transmembrane protein 155

208078_s_at	SNF1LK	SNF1-like kinase // SNF1-like kinase
217989_at	DHR58	dehydrogenase/reductase (SDR family) member 8
229125_at	ANKRD38	ankyrin repeat domain 38
205141_at	ANG // RNASE4	angiogenin, ribonuclease, RNase A family, 5 // ribonuclease, RNase A family, 4
204712_at	WIF1	WNT inhibitory factor 1
1552960_at	LRRC15	leucine rich repeat containing 15
225155_at	SNHG5	small nucleolar RNA host gene (non-protein coding) 5
204351_at	S100P	S100 calcium binding protein P
1569372_at	TUBB2B	Tubulin, beta 2B
205097_at	SLC26A2	solute carrier family 26 (sulfate transporter), member 2
204881_s_at	UGCG	UDP-glucose ceramide glucosyltransferase
203434_s_at	MME	membrane metallo-endopeptidase (neutral endopeptidase, enkephalinase)
1568574_x_at	SPP1	Secreted phosphoprotein 1 (osteopontin, bone sialoprotein I)
206908_s_at	CLDN11	claudin 11 (oligodendrocyte transmembrane protein)
1556153_s_at	NFKBIZ	Nuclear factor of kappa light polypeptide gene enhancer in B-cells inhibitor, zeta
210643_at	TNFSF11	tumor necrosis factor (ligand) superfamily, member 11, RANKL
203305_at	F13A1	coagulation factor XIII, A1 polypeptide
213791_at	PENK	proenkephalin
242324_x_at	CCBE1	collagen and calcium binding EGF domains 1
213338_at	TMEM158	transmembrane protein 158
213139_at	SNAI2	snail homolog 2 (Drosophila)
217979_at	TSPAN13	Tetraspanin 13
215420_at	IHH	Indian hedgehog homolog (Drosophila)
229645_at	C18orf51	chromosome 18 open reading frame 51
218717_s_at	LEPREL1	leprecan-like 1
238332_at	ANKRD29	ankyrin repeat domain 29
205828_at	MMP3	matrix metalloproteinase 3 (stromelysin 1, progelatinase)
209395_at	CHI3L1	chitinase 3-like 1 (cartilage glycoprotein-39)
204337_at	RGS4	regulator of G-protein signalling 4
201939_at	PLK2	polo-like kinase 2 (Drosophila)
228844_at	SLC13A5	solute carrier family 13 (sodium-dependent citrate transporter), member 5
218468_s_at	GREM1	gremlin 1, cysteine knot superfamily, homolog (Xenopus laevis)
201467_s_at	NQO1	NAD(P)H dehydrogenase, quinone 1
224482_s_at	RAB11FIP4	RAB11 family interacting protein 4 (class II)
206239_s_at	SPINK1	serine peptidase inhibitor, Kazal type 1
213492_at	COL2A1	collagen, type II, alpha 1
1552737_s_at	WWP2	WW domain containing E3 ubiquitin protein ligase 2
204162_at	KNTC2	kinetochore associated 2
213622_at	COL9A2	collagen, type IX, alpha 2
202497_x_at	SLC2A3	solute carrier family 2 (facilitated glucose transporter), member 3
206309_at	LECT1	leukocyte cell derived chemotaxin 1
1556427_s_at	LOC221091	similar to hypothetical protein
201762_s_at	PSME2	proteasome (prosome, macropain) activator subunit 2 (PA28 beta)
201795_at	LBR	lamin B receptor
209946_at	VEGFC	vascular endothelial growth factor C
210432_s_at	SCN3A	sodium channel, voltage-gated, type III, alpha
206439_at	DSPG3	dermatan sulfate proteoglycan 3
203498_at	DSCR1L1	Down syndrome critical region gene 1-like 1
202912_at	ADM	adrenomedullin
221729_at	COL5A2	collagen, type V, alpha 2
1555345_at	SLC38A4	solute carrier family 38, member 4
210095_s_at	IGFBP3	insulin-like growth factor binding protein 3
201601_x_at	IFITM1	interferon induced transmembrane protein 1 (9-27)
205483_s_at	ISG15	ISG15 ubiquitin-like modifier
1554685_a_at	KIAA1199	KIAA1199
221019_s_at	COLEC12	collectin sub-family member 12 // collectin sub-family member 12
240448_at	KIAA0802	KIAA0802
200790_at	ODC1	ornithine decarboxylase 1
206932_at	CH25H	cholesterol 25-hydroxylase
205352_at	SERPINI1	serpin peptidase inhibitor, clade I (neuroserpin), member 1
228640_at	---	CDNA clone IMAGE:4800096
205051_s_at	KIT	v-kit Hardy-Zuckerman 4 feline sarcoma viral oncogene homolog
204731_at	TGFBR3	transforming growth factor, beta receptor III (betaglycan, 300kDa)

221823_at	C5orf30	chromosome 5 open reading frame 30
1554736_at	ARHGAP29	Rho GTPase activating protein 29
217997_at	PHLDA1	pleckstrin homology-like domain, family A, member 1
226907_at	PPP1R14C	protein phosphatase 1, regulatory (inhibitor) subunit 14C
223235_s_at	SMOC2	SPARC related modular calcium binding 2
202403_s_at	COL1A2	collagen, type I, alpha 2
204469_at	PTPRZ1	protein tyrosine phosphatase, receptor-type, Z polypeptide 1
223614_at	C8orf57	chromosome 8 open reading frame 57
212850_s_at	LRP4	low density lipoprotein receptor-related protein 4
202965_s_at	CAPN6	calpain 6
223316_at	CCDC3	coiled-coil domain containing 3
200974_at	ACTA2	actin, alpha 2, smooth muscle, aorta
213293_s_at	TRIM22	tripartite motif-containing 22
222020_s_at	HNT	neurotrimin
210609_s_at	TP53I3	tumor protein p53 inducible protein 3
201739_at	SGK	serum/glucocorticoid regulated kinase
217995_at	SQRDL	sulfide quinone reductase-like (yeast)
204682_at	LTBP2	latent transforming growth factor beta binding protein 2
201195_s_at	SLC7A5	solute carrier family 7 (cationic amino acid transporter, y+ system), member 5
206764_x_at	MPPE1	metallophosphoesterase 1
213060_s_at	CHI3L2	chitinase 3-like 2 /// chitinase 3-like 2
205334_at	S100A1	S100 calcium binding protein A1
209955_s_at	FAP	fibroblast activation protein, alpha
204035_at	SCG2	secretogranin II (chromogranin C)
217875_s_at	TMEPAI	transmembrane, prostate androgen induced RNA
203879_at	PIK3CD	phosphoinositide-3-kinase, catalytic, delta polypeptide
202709_at	FMOD	fibromodulin
1554737_at	FBN2	fibrillin 2 (congenital contractural arachnodactyly)
205941_s_at	COL10A1	collagen, type X, alpha 1 (Schmid metaphyseal chondrodysplasia)
202727_s_at	IFNGR1	interferon gamma receptor 1
226930_at	FNDC1	fibronectin type III domain containing 1
207001_x_at	TSC22D3	TSC22 domain family, member 3
206960_at	GPR23	G protein-coupled receptor 23
203666_at	CXCL12	chemokine (C-X-C motif) ligand 12 (stromal cell-derived factor 1)
204320_at	COL11A1	collagen, type XI, alpha 1
203058_s_at	PAPSS2	3'-phosphoadenosine 5'-phosphosulfate synthase 2
205870_at	BDKRB2	bradykinin receptor B2
201464_x_at	JUN	v-jun sarcoma virus 17 oncogene homolog (avian)
226989_at	RGMB	RGM domain family, member B
229740_at	LOC643008	PP12104
203304_at	BAMBI	BMP and activin membrane-bound inhibitor homolog ( <i>Xenopus laevis</i> )
218899_s_at	BALCL	brain and acute leukemia, cytoplasmic
224348_s_at	H19	H19, imprinted maternally expressed untranslated mRNA
209560_s_at	DLK1	delta-like 1 homolog ( <i>Drosophila</i> )
222162_s_at	ADAMTS1	ADAM metalloproteinase with thrombospondin type 1 motif, 1
206115_at	EGR3	early growth response 3
1562094_at	MGC26963	Hypothetical protein MGC26963
216952_s_at	LMNB2	lamin B2
210948_s_at	LEF1	lymphoid enhancer-binding factor 1
1563466_at	MYLK	Myosin, light polypeptide kinase
212689_s_at	JMJD1A	jumonji domain containing 1A
205347_s_at	TM6SL8	thymosin-like 8
204967_at	SHROOM2	shroom family member 2
218009_s_at	PRC1	protein regulator of cytokinesis 1
212067_s_at	C1R /// LOC643676	complement component 1, r subcomponent
1560259_at	RORA	RAR-related orphan receptor A
206432_at	HAS2	hyaluronan synthase 2
1561065_at	ANKRD6	Ankyrin repeat domain 6
1555800_at	ZNF533	zinc finger protein 533
219747_at	C4orf31	chromosome 4 open reading frame 31
1558636_s_at	ADAMTS5	ADAM metalloproteinase with thrombospondin type 1 motif, 5 (aggrecanase-2)
227497_at	---	CDNA FLJ11723 fis, clone HEMBA1005314
1555527_at	COL9A1	collagen, type IX, alpha 1

202768_at	FOSB	FBJ murine osteosarcoma viral oncogene homolog B
204221_x_at	GLIPR1	GLI pathogenesis-related 1 (glioma)
204774_at	EVI2A	ecotropic viral integration site 2A
206157_at	PTX3	pentraxin-related gene, rapidly induced by IL-1 beta
202643_s_at	TNFAIP3	tumor necrosis factor, alpha-induced protein 3
234994_at	KIAA1913	KIAA1913
227475_at	FOXQ1	forkhead box Q1
219334_s_at	OBFC2A	oligonucleotide/oligosaccharide-binding fold containing 2A
218986_s_at	FLJ20035	hypothetical protein FLJ20035
228382_at	FAM105B	family with sequence similarity 105, member B
205523_at	HAPLN1	hyaluronan and proteoglycan link protein 1
224967_at	UGCG	UDP-glucose ceramide glucosyltransferase
213817_at	---	CDNA FLJ13601 fis, clone PLACE1010069
212900_at	SEC24A	SEC24 related gene family, member A (S. cerevisiae)
1552619_a_at	ANLN	anillin, actin binding protein
224609_at	SLC44A2	solute carrier family 44, member 2
203755_at	BUB1B	BUB1 budding uninhibited by benzimidazoles 1 homolog beta (yeast)
1555724_s_at	TAGLN	transgelin
202450_s_at	CTSK	cathepsin K (pyncnodysostosis)
213861_s_at	FAM119B	family with sequence similarity 119, member B
213248_at	LOC221362	hypothetical protein LOC221362
203570_at	LOXL1	lysyl oxidase-like 1
230407_at	---	Transcribed locus, strongly similar to strawberry notch homolog 1; MOP-3
209567_at	RRS1	RRS1 ribosome biogenesis regulator homolog (S. cerevisiae)
210512_s_at	VEGF	vascular endothelial growth factor
205289_at	BMP2	bone morphogenetic protein 2
203065_s_at	CAV1	caveolin 1, caveolae protein, 22kDa
203758_at	CTSO	cathepsin O
205476_at	CCL20	chemokine (C-C motif) ligand 20
207826_s_at	ID3	inhibitor of DNA binding 3, dominant negative helix-loop-helix protein
205479_s_at	PLAU	plasminogen activator, urokinase
201136_at	PLP2	proteolipid protein 2 (colonic epithelium-enriched)
203764_at	DLG7	discs, large homolog 7 (Drosophila)
209160_at	AKR1C3	aldo-keto reductase family 1, member C3 (3-alpha hydroxysteroid dehydrogenase, type II)
207977_s_at	DPT	dermatopontin
205125_at	PLCD1	phospholipase C, delta 1
207980_s_at	CITED2	Cbp/p300-interacting transactivator, with Glu/Asp-rich carboxy-terminal domain, 2
204475_at	MMP1	matrix metalloproteinase 1 (interstitial collagenase)
1556209_at	CLEC2B	C-type lectin domain family 2, member B
205830_at	CLGN	calmegin
219295_s_at	PCOLCE2	procollagen C-endopeptidase enhancer 2
205907_s_at	OMD	osteomodulin
206869_at	CHAD	chondroadherin
223836_at	KSP37	Ksp37 protein
204948_s_at	FST	folistatin
240955_at	PANX3	pannexin 3

## References

1. **Chagin AS, Savendahl L** 2007 Estrogens and growth: review. *Pediatr Endocrinol Rev* 4: 329-334
2. **Nilsson O, Chrysis D, Pajulo O, Boman A, Holst M, Rubinstein J, Martin RE, Savendahl L** 2003 Localization of estrogen receptors-alpha and -beta and androgen receptor in the human growth plate at different pubertal stages. *J Endocrinol* 177:319-326
3. **Vidal O, Lindberg MK, Hollberg K, Baylink DJ, Andersson G, Lubahn DB, Mohan S, Gustafsson JA, Ohlsson C** 2000 Estrogen receptor specificity in the regulation of skeletal growth and maturation in male mice. *Proc Natl Acad Sci U S A* 97:5474-5479
4. **Smith EP, Boyd J, Frank GR, Takahashi H, Cohen RM, Specker B, Williams TC, Lubahn DB, Korach KS** 1994 Estrogen resistance caused by a mutation in the estrogen-receptor gene in a man. *N Engl J Med* 331:1056-1061
5. **Pelttari K, Steck E, Richter W** 2008 The use of mesenchymal stem cells for chondrogenesis. *Injury* 39 Suppl 1:S58-S65
6. **Bernardo ME, Emons JA, Karperien M, Nauta AJ, Willemze R, Roelofs H, Romeo S, Marchini A, Rappold GA, Vukicevic S, Locatelli F, Fibbe WE** 2007 Human mesenchymal stem cells derived from bone marrow display a better chondrogenic differentiation compared with other sources. *Connect Tissue Res* 48:132-140
7. **Djouad F, Delorme B, Maurice M, Bony C, Apparailly F, Louis-Pleunce P, Canovas F, Charbord P, Noel D, Jorgensen C** 2007 Microenvironmental changes during differentiation of mesenchymal stem cells towards chondrocytes. *Arthritis Res Ther* 9:R33
8. **Larson BL, Ylostalo J, Prockop DJ** 2008 Human multipotent stromal cells undergo sharp transition from division to development in culture. *Stem Cells* 26:193-201
9. **Mrugala D, Dossat N, Ringe J, Delorme B, Coffy A, Bony C, Charbord P, Haupl T, Daures JP, Noel D, Jorgensen C** 2009 Gene Expression Profile of Multipotent Mesenchymal Stromal Cells: Identification of Pathways Common to TGFbeta3/BMP2-Induced Chondrogenesis. *Cloning Stem Cells*
10. **Phinney DG, Prockop DJ** 2007 Concise review: mesenchymal stem/multipotent stromal cells: the state of transdifferentiation and modes of tissue repair--current views. *Stem Cells* 25:2896-2902
11. **Sekiya I, Vuoristo JT, Larson BL, Prockop DJ** 2002 In vitro cartilage formation by human adult stem cells from bone marrow stroma defines the sequence of cellular and molecular events during chondrogenesis. *Proc Natl Acad Sci U S A* 99:4397-4402

12. **Sekiya I, Larson BL, Smith JR, Pochampally R, Cui JG, Prockop DJ** 2002 Expansion of human adult stem cells from bone marrow stroma: conditions that maximize the yields of early progenitors and evaluate their quality. *Stem Cells* 20:530-541
13. **Shahdadfar A, Fronsdal K, Haug T, Reinholt FP, Brinchmann JE** 2005 In vitro expansion of human mesenchymal stem cells: choice of serum is a determinant of cell proliferation, differentiation, gene expression, and transcriptome stability. *Stem Cells* 23:1357-1366
14. **Ylostalo J, Smith JR, Pochampally RR, Matz R, Sekiya I, Larson BL, Vuoristo JT, Prockop DJ** 2006 Use of differentiating adult stem cells (marrow stromal cells) to identify new downstream target genes for transcription factors. *Stem Cells* 24:642-652
15. **Goeman JJ, Buhlmann P** 2007 Analyzing gene expression data in terms of gene sets: methodological issues. *Bioinformatics* 23:980-987
16. **DeLise AM, Fischer L, Tuan RS** 2000 Cellular interactions and signaling in cartilage development. *Osteoarthritis Cartilage* 8:309-334
17. **Zelzer E, Olsen BR** 2005 Multiple roles of vascular endothelial growth factor (VEGF) in skeletal development, growth, and repair. *Curr Top Dev Biol* 65:169-187
18. **De LF, Barnes KM, Uyeda JA, De-Levi S, Abad V, Palese T, Mericq V, Baron J** 2001 Regulation of growth plate chondrogenesis by bone morphogenetic protein-2. *Endocrinology* 142:430-436
19. **Minina E, Wenzel HM, Kreschel C, Karp S, Gaffield W, McMahon AP, Vortkamp A** 2001 BMP and Ihh/PTHrP signaling interact to coordinate chondrocyte proliferation and differentiation. *Development* 128:4523-4534
20. **Buxton P, Edwards C, Archer CW, Francis-West P** 2001 Growth/differentiation factor-5 (GDF-5) and skeletal development. *J Bone Joint Surg Am* 83-A Suppl 1:S23-S30
21. **Funaba M, Ogawa K, Murata T, Fujimura H, Murata E, Abe M, Takahashi M, Torii K** 1996 Follistatin and activin in bone: expression and localization during endochondral bone development. *Endocrinology* 137:4250-4259
22. **Tuan RS** 2003 Cellular signaling in developmental chondrogenesis: N-cadherin, Wnts, and BMP-2. *J Bone Joint Surg Am* 85-A Suppl 2:137-141
23. **Bluteau G, Julien M, Magne D, Mallein-Gerin F, Weiss P, Daculsi G, Guicheux J** 2007 VEGF and VEGF receptors are differentially expressed in chondrocytes. *Bone* 40:568-576
24. **Maes C, Stockmans I, Moermans K, Van LR, Smets N, Carmeliet P, Bouillon R, Carmeliet G** 2004 Soluble VEGF isoforms are essential for establishing epiphyseal vascularization and regulating chondrocyte development and survival. *J Clin Invest* 113:188-199

25. **Mayer H, Bertram H, Lindenmaier W, Korff T, Weber H, Weich H** 2005 Vascular endothelial growth factor (VEGF-A) expression in human mesenchymal stem cells: autocrine and paracrine role on osteoblastic and endothelial differentiation. *J Cell Biochem* 95:827-839
26. **Clark K, Langeslag M, Figdor CG, van Leeuwen FN** 2007 Myosin II and mechanotransduction: a balancing act. *Trends Cell Biol* 17:178-186
27. **Howe A, Aplin AE, Alahari SK, Juliano RL** 1998 Integrin signaling and cell growth control. *Curr Opin Cell Biol* 10:220-231
28. **Ulici V, Hoenselaar KD, Gillespie JR, Beier F** 2008 The PI3K pathway regulates endochondral bone growth through control of hypertrophic chondrocyte differentiation. *BMC Dev Biol* 8:40
29. **Johnson K, Hashimoto S, Lotz M, Pritzker K, Terkeltaub R** 2001 Interleukin-1 induces pro-mineralizing activity of cartilage tissue transglutaminase and factor XIIIa. *Am J Pathol* 159:149-163
30. **Nurminskaya MV, Linsenmayer TF** 2002 Immunohistological analysis of transglutaminase factor XIIIa expression in mouse embryonic growth plate. *J Orthop Res* 20:575-578
31. **Aeschlimann D, Mosher D, Paulsson M** 1996 Tissue transglutaminase and factor XIII in cartilage and bone remodeling. *Semin Thromb Hemost* 22:437-443
32. **Madsen CD, Sidenius N** 2008 The interaction between urokinase receptor and vitronectin in cell adhesion and signalling. *Eur J Cell Biol* 87:617-629
33. **Sakiyama H, Nakagawa K, Kuriwa K, Imai K, Okada Y, Tsuchida T, Moriya H, Imajoh-Ohmi S** 1997 Complement C1s, a classical enzyme with novel functions at the endochondral ossification center: immunohistochemical staining of activated C1s with a neoantigen-specific antibody. *Cell Tissue Res* 288:557-565
34. **Weber KT, Sun Y, Tyagi SC, Cleutjens JP** 1994 Collagen network of the myocardium: function, structural remodeling and regulatory mechanisms. *J Mol Cell Cardiol* 26:279-292
35. **Bauer PM, Yu J, Chen Y, Hickey R, Bernatchez PN, Looft-Wilson R, Huang Y, Giordano F, Stan RV, Sessa WC** 2005 Endothelial-specific expression of caveolin-1 impairs microvascular permeability and angiogenesis. *Proc Natl Acad Sci U S A* 102:204-209
36. **Galbiati F, Volonte D, Brown AM, Weinstein DE, Ben-Ze'ev A, Pestell RG, Lisanti MP** 2000 Caveolin-1 expression inhibits Wnt/beta-catenin/Lef-1 signaling by recruiting beta-catenin to caveolae membrane domains. *J Biol Chem* 275:23368-23377
37. **Grande-Garcia A, del Pozo MA** 2008 Caveolin-1 in cell polarization and directional migration. *Eur J Cell Biol* 87:641-647
38. **Jasmin JF, Mercier I, Sotgia F, Lisanti MP** 2006 SOCS proteins and caveolin-1 as negative regulators of endocrine signaling. *Trends Endocrinol Metab* 17:150-158



39. **Gagarina V, Carlberg AL, Pereira-Mouries L, Hall DJ** 2008 Cartilage oligomeric matrix protein protects cells against death by elevating members of the IAP family of survival proteins. *J Biol Chem* 283:648-659
40. **Hirsch E, Costa C, Cirao E** 2007 Phosphoinositide 3-kinases as a common platform for multi-hormone signaling. *J Endocrinol* 194:243-256
41. **Miettinen M, Lasota J** 2005 KIT (CD117): a review on expression in normal and neoplastic tissues, and mutations and their clinicopathologic correlation. *Appl Immunohistochem Mol Morphol* 13:205-220
42. **Constantinescu D, Gray HL, Sammak PJ, Schatten GP, Csoka AB** 2006 Lamin A/C expression is a marker of mouse and human embryonic stem cell differentiation. *Stem Cells* 24:177-185
43. **Heinrichs C, Yanovski JA, Roth AH, Yu YM, Domene HM, Yano K, Cutler GB, Jr, Baron J** 1994 Dexamethasone increases growth hormone receptor messenger ribonucleic acid levels in liver and growth plate. *Endocrinology* 135:1113-1118
44. **Dai M, Wang P, Boyd AD, Kostov G, Athey B, Jones EG, Bunney WE, Myers RM, Speed TP, Akil H, Watson SJ, Meng F** 2005 Evolving gene/transcript definitions significantly alter the interpretation of GeneChip data. *Nucleic Acids Res* 33:e175
45. **Chu TM, Weir B, Wolfinger R** 2002 A systematic statistical linear modeling approach to oligonucleotide array experiments. *Math Biosci* 176:35-51